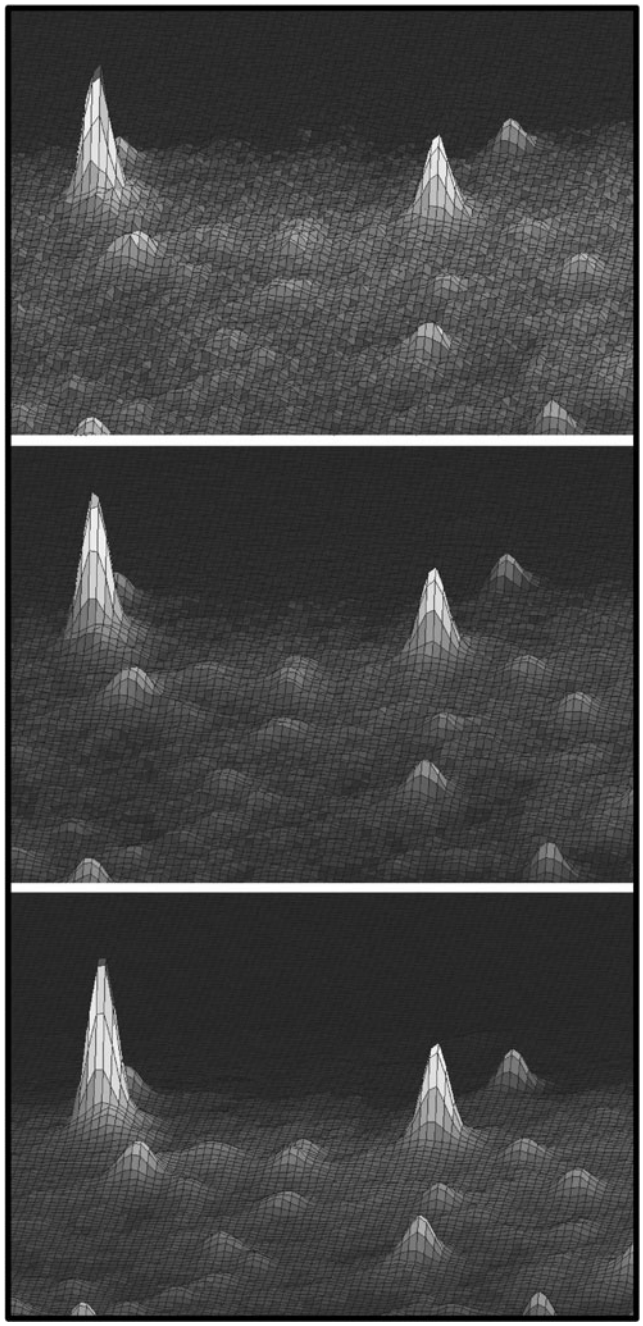

Supplementary Figure 1. Increase of the signal-to-noise ratio by smoothing. A TIRF image of an insulin-secreting MIN6 cell with granules labeled by insulin-EGFP is shown as a surface plot of the raw data (upper image), the result of a 2D convolution (middle image) and the result of a 3D convolution (lower image).

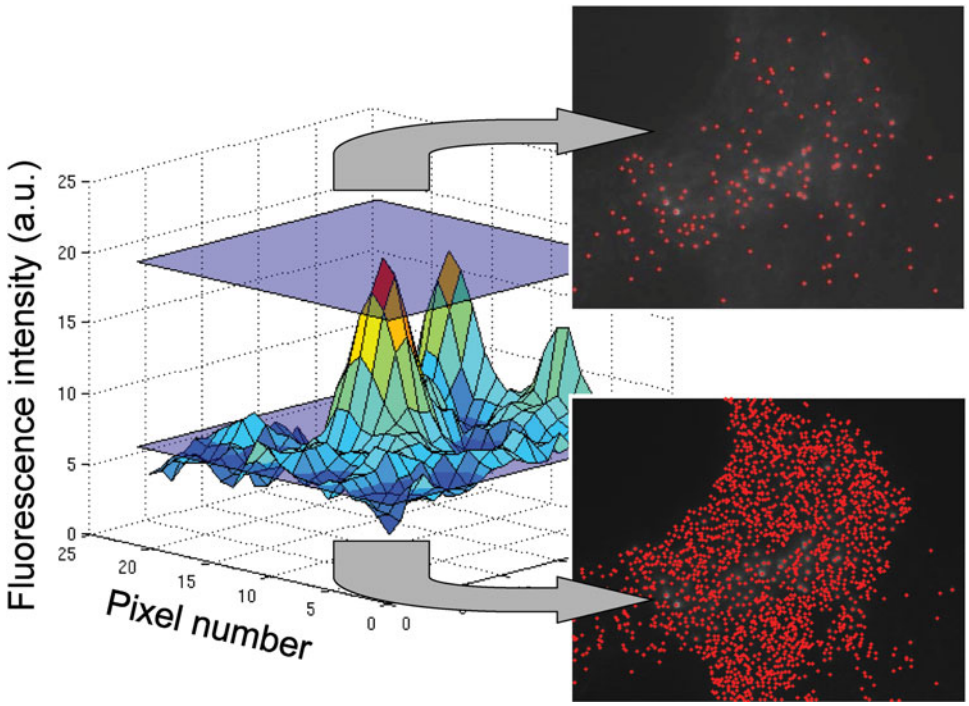

Supplementary Figure 2. Granule detection by setting a noise-dependent threshold. When all local intensity maxima of the respective frame were accepted as peaks, this resulted in the complete filling of the cell contour (lower right inset). When only local maxima were accepted that were above a certain signal-to-noise ratio, the resulting removal of the weak fluorescent spots reduced the number of objects from approximately 15,000 to approximately 100 (upper right inset). This corresponds to the removal of low frequency noise and gave stable results when the threshold was set at a signal-to-noise ratio of two.

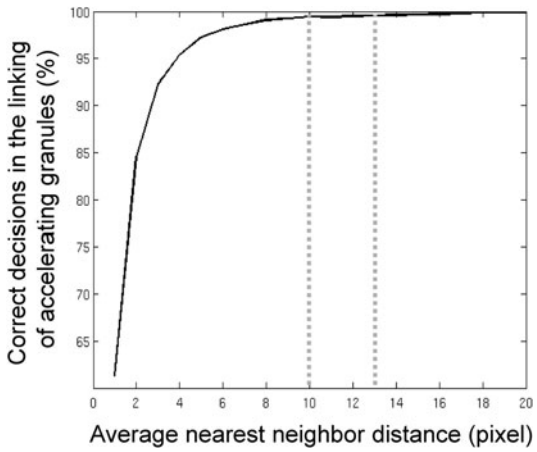

Supplementary Figure 3. Correct linking of fast granules by flexible adaption of the gating distance. Simulated granules were programmed to have a caging diameter between 0.5 and 4 pixels with few outlier granules having maximal values of 16 pixels. The black line gives the percentage of correct linking in dependence on the average nearest neighbor distance of the objects. At a distance of 1 pixel, only 60% of the accelerating granules were correctly tracked, whereas a value of 8 resulted in more than 99% correct decisions. The dotted lines indicate the range of the average nearest neighbor distances in the original sequences.

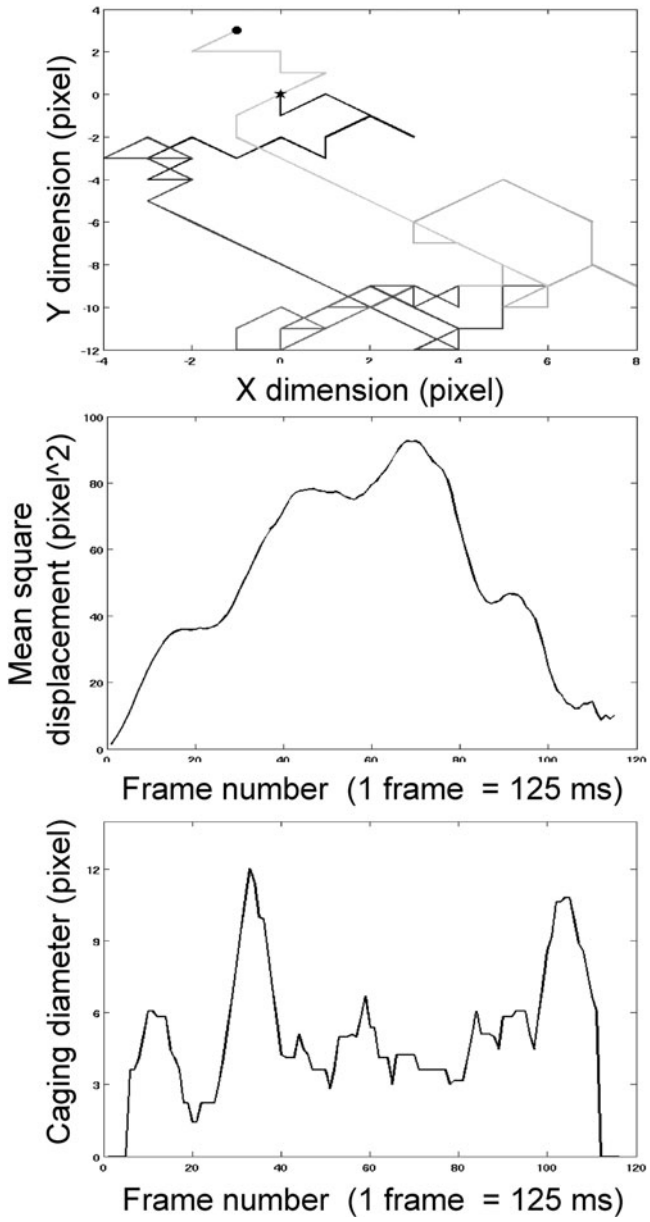

Supplementary Figure 4. Comparison of the mean square displacement (MSD) and the caging diameter (CD) as methods to describe granule mobility in the *X-Y* dimension. A granule itinerary containing phases of random and non-random mobility was simulated. The beginning is marked by an asterisk, the end by a filled circle (upper graph). The resulting MSD plot leaves ample space for subjective interpretations. The criterion of linearity can be fulfilled or missed just by variation of the evaluation time interval (middle graph). The CD derived from the same set of data permits to localize the two phases of non-random mobility against the background of random behaviour (lower graph).

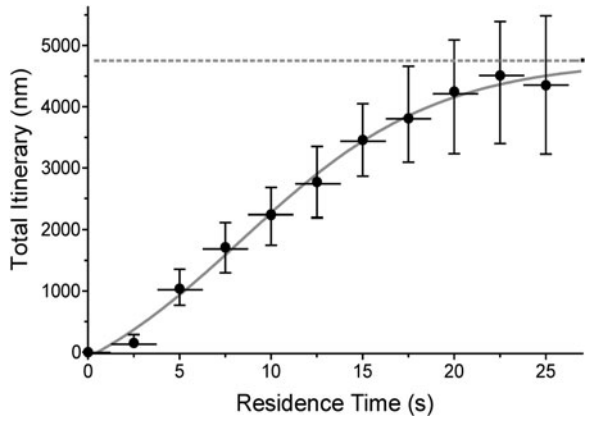

Supplementary Figure 5. Mobility of insulin secretory granules in the *X-Y* dimension. After removal of all granules that were present for only one image the residence time of all other granules was subdivided into 10 groups of 20 images each (equivalent to 2.5 s per group). Shown is the time-dependent increase in the length of the total itineraries (for the original data see Fig. 5a, upper panel) after transformation of the values into means ± SEM. The horizontal bars indicate that the means were calculated from the data collected during 2.5 s intervals. Using a double sigmoidal curve fit (r^2 = 0.99) an upper limit of the total itineraries of 4,763 ± 237 nm (dotted line) was calculated. The data were derived from four experiments.

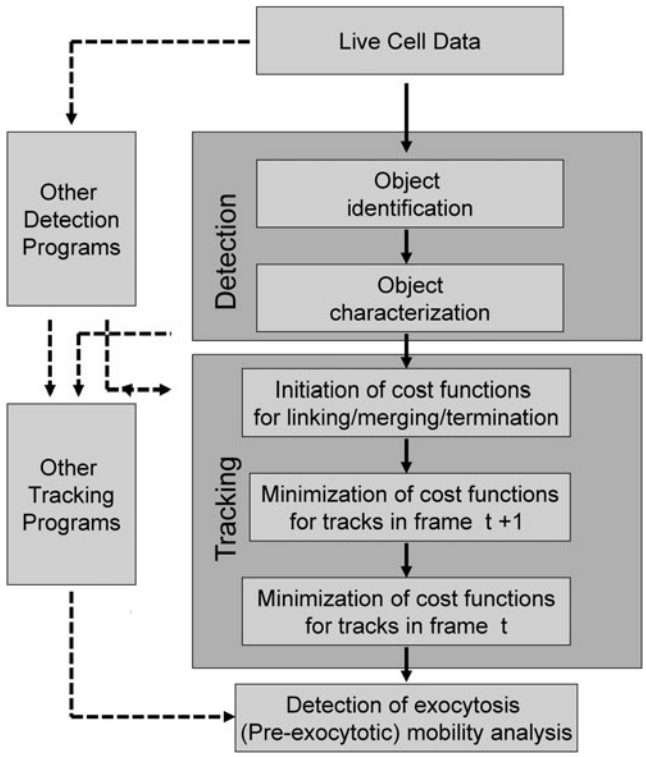

Supplementary Figure 6. Overview on the program structure to link observer-independent detection of exocytosis with granule tracking. Detection and tracking are separate processes, permitting the import of data sets on detected granules or the export of tracking data for evaluation by other programs. Tracks are constructed by different decision criteria (cf. text). In combination with the detection of exocytosis, the prefusion mobility can be compared with the behavior of nonfusing granules.